Reaction rates for a generalized reaction-diffusion master equation

Stefan Hellander* and Linda Petzold
Department of Computer Science, University of California, Santa Barbara, Santa Barbara, California 93106-5070, USA
(Received 25 March 2015; revised manuscript received 2 September 2015; published 19 January 2016)

It has been established that there is an inherent limit to the accuracy of the reaction-diffusion master equation. Specifically, there exists a fundamental lower bound on the mesh size, below which the accuracy deteriorates as the mesh is refined further. In this paper we extend the standard reaction-diffusion master equation to allow molecules occupying neighboring voxels to react, in contrast to the traditional approach, in which molecules react only when occupying the same voxel. We derive reaction rates, in two dimensions as well as three dimensions, to obtain an optimal match to the more fine-grained Smoluchowski model and show in two numerical examples that the extended algorithm is accurate for a wide range of mesh sizes, allowing us to simulate systems that are intractable with the standard reaction-diffusion master equation. In addition, we show that for mesh sizes above the fundamental lower limit of the standard algorithm, the generalized algorithm reduces to the standard algorithm. We derive a lower limit for the generalized algorithm which, in both two dimensions and three dimensions, is of the order of the reaction radius of a reacting pair of molecules.

DOI: 10.1103/PhysRevE.93.013307

I. INTRODUCTION

Stochastic modeling has become a ubiquitous tool in the study of biochemical reaction networks [1–5], as the traditional approach of deterministic modeling has been shown to be unsuitable for some systems where species are present in low copy numbers or systems with spatial inhomogeneities [3,6]. Instead stochastic, spatially homogenous or inhomogeneous, models are employed.

Stochastic modeling can be carried out on multiple different scales. For processes occurring on the time scales typical of living cells we consider three modeling scales: the spatially homogeneous well-mixed scale, the mesoscopic spatially heterogeneous scale, and the microscopic particle-tracking scale. In this paper the focus is on spatially heterogeneous modeling.

A prevalent model on the mesoscopic scale is the standard reaction-diffusion master equation (RDME), in which diffusion of individual molecules is modeled by discrete jumps between voxels, while reactions occur at a given intensity once molecules occupy the same voxel. The next subvolume method (NSM) [7] is an efficient algorithm for generating single trajectories of the system. The NSM has been implemented in several software packages, including URDME [8], PyURDME [9], STEPS [10], and MesoRD [11]. It is also available as a part of larger simulation frameworks such as StochSS (www.stochss.org) and E-Cell [12].

On the microscopic scale we model the molecules as hard spheres moving by normal diffusion. We track the continuous position of individual molecules, and molecules react with a probability upon collision. This model is commonly referred to as the Smoluchowski model [13], with the addition of a Robin boundary condition at the reaction radius of a pair of molecules. Algorithms aimed at accurately and efficiently simulating the Smoluchowski model for general systems have been implemented in E-Cell [12], Smoldyn [14], and MCell [15].

*st.hellander@gmail.com

It has previously been shown that there is an inherent bound of several reaction radii on the spatial accuracy of the standard RDME compared to the Smoluchowski model [16,17]. It was shown in [17] that by choosing correct mesoscopic reaction rates, the standard RDME could be made accurate all the way down to this lower bound. However, for mesh resolutions below this lower bound, the accuracy deteriorates.

In this paper we generalize the standard RDME by allowing molecules occupying neighboring voxels to react. Henceforth we refer to this generalization as the *generalized RDME*. The acronym RDME usually refers to the standard RDME, but to minimize the possibility of confusion as to which of the algorithms we are referring to, we adopt the acronym sRDME for the standard RDME and gRDME for the generalized RDME. Similar generalizations have been considered previously in [18] and [19]. In [17], Isaacson discretizes the Doi model [20] to obtain a convergent RDME. In [19], reaction rates are derived for a spherical model and applied to the RDME on a Cartesian mesh. In this paper we take a fundamentally different approach. By deriving reaction rates to match certain statistics of the Smoluchowski model, we arrive at analytical expressions for the reaction rates and show that this approach yields accurate results down to a fundamental lower limit on the mesh size. This mesh size will be of the order of the reaction radius of two molecules.

Importantly, we derive reaction rates under specific assumptions about the dynamics of dissociating molecules, and we show with a simple example that not doing so may lead to reaction rates that are inaccurate for certain systems. We thus argue that it is crucial to take dissociations into account in the derivation of reaction rates for the gRDME.

The outline of the paper is as follows. In Sec. II we review the Smoluchowski model and the sRDME and how they are connected through the mesoscopic reaction rates. In Sec. III we describe the generalized algorithm and derive accurate mesoscopic reaction rates as well as the lower limit on the mesh size. Finally, in Sec. IV, we study two numerical examples, demonstrating the accuracy of the gRDME and how it can be used to simulate systems that are intractable with the sRDME.

II. BACKGROUND

A. Microscopic level

At this level of modeling we track the continuous position of individual molecules, modeled by hard spheres and moving by normal diffusion. Each species S_i has a diffusion constant D_i and a radius of σ_i, called the reaction radius. Consider two molecules, one of species S_1 and one of species S_2, with positions $\mathbf{x}_{1n}$ and $\mathbf{x}_{2n}$ at time t_n. The molecules can react according to $S_1 + S_2 \underset{k_d}{\overset{k_a}{\rightleftarrows}} S_3$, where S_3 is some product. The probability distribution function $p(\mathbf{x}_1,\mathbf{x}_2,t|\mathbf{x}_{1n},\mathbf{x}_{2n},t_n)$ represents the probability that the positions of the molecules are given by $\mathbf{x}_1$ and $\mathbf{x}_2$ at time t; p then satisfies the Smoluchowski equation

$$\partial_t p = D_1 \Delta_{\mathbf{x}_1} p + D_2 \Delta_{\mathbf{x}_2} p, \tag{1}$$

with the reactive Robin boundary condition

$$K \frac{\partial p_{\mathbf{x}_2-\mathbf{x}_1}}{\partial n}\bigg|_{\|\mathbf{x}_2-\mathbf{x}_1\|=\sigma} = k_a\, p(\|\mathbf{x}_2-\mathbf{x}_1\|=\sigma,t), \tag{2}$$

where $D = D_1 + D_2$, $\sigma = \sigma_1 + \sigma_2$ is the sum of the reaction radii, k_a is the microscopic reaction rate, and

$$K = \begin{cases} 2\pi\sigma D & \text{(2D)}, \\ 4\pi\sigma^2 D & \text{(3D)}. \end{cases} \tag{3}$$

The initial condition is given by

$$p(\mathbf{x}_2-\mathbf{x}_1,t_n) = \delta((\mathbf{x}_2-\mathbf{x}_1)-(\mathbf{x}_{2n}-\mathbf{x}_{1n})), \tag{4}$$

and since we assume that there is no outer boundary, we enforce $p(\|\mathbf{x}_2-\mathbf{x}_1\|\to\infty,t)=0$.

It can be shown that with the change of variables

$$\mathbf{Y} = \sqrt{\frac{D_2}{D_1}}\mathbf{x}_1 + \sqrt{\frac{D_1}{D_2}}\mathbf{x}_2, \tag{5}$$

$$\mathbf{y} = \mathbf{x}_2 - \mathbf{x}_1, \tag{6}$$

we obtain two independent equations, where the equation for $\mathbf{Y}$ describes free diffusion, while the equation for $\mathbf{y}$ becomes

$$\partial_t p(\mathbf{y},t) = D\Delta_{\mathbf{y}} p(\mathbf{y},t), \tag{7}$$

with the boundary condition

$$K \frac{\partial p_{\mathbf{y}}}{\partial n}\bigg|_{\|\mathbf{y}\|=\sigma} = k_a\, p_{\mathbf{y}}(\|\mathbf{y}\|=\sigma,t). \tag{8}$$

The initial condition becomes $p_{\mathbf{y}}(\mathbf{y},t_n) = \delta(\mathbf{y}-\mathbf{y}_n)$, and the outer boundary condition is now $p_{\mathbf{y}}(\|\mathbf{y}\|\to\infty,t)=0$. This equation can be solved analytically in three dimensions [21], but the solution is difficult and expensive to evaluate numerically. Applying an operator split method to (7) and (8) can significantly simplify the process of sampling new positions from the probability density function [22].

An S_3 molecule is assumed to dissociate according to an exponential distribution with the mean k_d. Following a dissociation, the two products S_1 and S_2 are placed in contact a distance of σ apart.

A system of more than two molecules is not amenable to the direct approach of solving for the full probability density function, due to the high dimensionality of the problem. A common approach is instead to approximate the full problem as a set of one- and two-body problems, by dividing the system into subsets of single and pairs of molecules according to the distances between them. We can obtain a good approximation of the full problem by updating each subset independently during short time steps Δt. This algorithm is called the Green's function reaction dynamics (GFRD) [23,24], and all microscale computations in this paper are carried out using a variant of the GFRD algorithm [22].

B. Standard reaction-diffusion master equation

At the mesoscopic scale the simulation domain is discretized by N nonoverlapping voxels, and diffusion is modeled as discrete jumps between the nodes of the voxels. The mesh may be either a Cartesian mesh or an unstructured, tetrahedral (three-dimensional; 3D), or triangular (two-dimensional; 2D) mesh. A Cartesian mesh is suitable if the domain is simple, for instance, a square or a cube, while an unstructured mesh has advantages for complicated domains. The jump coefficients between voxels are given by $2D/h^2$ in the case of a Cartesian mesh, where h is the width of a voxel and D the diffusion rate of the molecule. For an unstructured mesh, the jump coefficients can be obtained from a finite-element discretization of the diffusion equation [25]. Reactions occur with some intensity when molecules occupy the same voxel.

Let $p(\mathbf{x},t|\mathbf{x}_n,t_n)$ be the probability that the system is found in state $\mathbf{x}$ at time t, given that it was in state $\mathbf{x}_n$ at time t_n. For brevity of notation, let $p(\mathbf{x},t) = p(\mathbf{x},t|\mathbf{x}_n,t_n)$. Let $\mathbf{x}_{i\cdot}$ and $\mathbf{x}_{\cdot j}$ denote the ith row and the jth column of the $N\times S$ state matrix $\mathbf{x}$, respectively, where S is the number of species of the system. The sRDME is given by

$$\begin{aligned}\frac{\mathrm{d}}{\mathrm{d}t}p(\mathbf{x},t) &= \sum_{i=1}^{N}\sum_{r=1}^{M} a_{ir}(\mathbf{x}_{i\cdot}-\boldsymbol{\mu}_{ir})p(\mathbf{x}_{1\cdot},\ldots,\mathbf{x}_{i\cdot}-\boldsymbol{\mu}_{ir},\ldots,\mathbf{x}_{N\cdot},t) \\ &\quad - \sum_{i=1}^{N}\sum_{r=1}^{M} a_{ir}(\mathbf{x}_{i\cdot})p(\mathbf{x},t) \\ &\quad + \sum_{j=1}^{S}\sum_{i=1}^{N}\sum_{k=1}^{N} d_{jik}(\mathbf{x}_{\cdot j}-\boldsymbol{\nu}_{ijk})p(\mathbf{x}_{\cdot 1},\ldots,\mathbf{x}_{\cdot j}-\boldsymbol{\nu}_{ijk},\ldots,\mathbf{x}_{\cdot S},t) \\ &\quad - \sum_{j=1}^{S}\sum_{i=1}^{N}\sum_{k=1}^{N} d_{ijk}(\mathbf{x}_{\cdot j})p(\mathbf{x},t),\end{aligned} \tag{9}$$

where the propensity functions of the M chemical reactions are denoted $a_{ir}(\mathbf{x}_i)$, $\boldsymbol{\mu}_{ir}$ are the stoichiometry vectors associated with the reactions, d_{ijk} are the jump coefficients, and $\boldsymbol{\nu}_{ijk}$ are stoichiometry vectors for diffusion events.

The sRDME is in general too high-dimensional to be solved by direct approaches. An alternative approach is to generate individual trajectories of the system with stochastic simulations. The NSM [7] is an efficient algorithm frequently used for that purpose.

C. Reaction rates for the standard reaction-diffusion master equation

Consider a system of two molecules, one of species S_1 and one of species S_2, that react according to $S_1 + S_2 \underset{k_d}{\overset{k_a}{\rightleftarrows}} S_3$, where k_a and k_d are the microscopic reaction rates. Assume that the molecules diffuse in a square (2D) or cube (3D) with periodic boundary conditions. Without loss of generality, assume that the S_1 molecule is fixed at the origin and that the S_2 molecule diffuses freely at a diffusion rate D. The S_2 molecule is initialized according to a uniform distribution.

Let $\tau_{\text{meso}}(k_a^{\text{meso}},h)$ be the mean association time of the two molecules on the mesoscopic scale, and let $\tau_{\text{micro}}(k_a)$ be the mean association time on the microscopic scale. Under the assumption that $\tau_{\text{meso}}(k_a^{\text{meso}},h) = \tau_{\text{micro}}(k_a)$ holds, it is shown in [16] and [17] that the mesoscopic association rate is given by

$$k_a^{\text{meso}} = \rho^{(d)}(k_a,h) = \frac{k_a}{h^d}\left[1 + \frac{k_a}{D}G^{(d)}(h,\sigma)\right]^{-1}, \tag{10}$$

where d is the dimension,

$$G^{(d)}(h,\sigma) = \begin{cases} \frac{1}{2\pi}\ln\left(\pi^{-\frac{1}{2}}\frac{h}{\sigma}\right) - \frac{1}{4}\left(\frac{3}{2\pi} + C_2\right) & \text{(2D)}, \\ \frac{1}{4\pi\sigma} - \frac{C_3}{6h} & \text{(3D)}, \end{cases} \tag{11}$$

and

$$C_d \approx \begin{cases} 0.1951, & d = 2, \\ 1.5164, & d = 3. \end{cases} \tag{12}$$

The microscopic parameters are σ, the sum of the reaction radii of the molecules, D, the sum of the diffusion constants, and k_a, the microscopic reaction rate. To simplify the notation somewhat, we let $\tau^{\rho}_{\text{meso}}(k_a,h) := \tau_{\text{meso}}(\rho^{(d)}(k_a,h),h)$. For a reversible reaction we match the mean binding time for $h > h^*_\infty$, where

$$h^*_\infty \approx \begin{cases} \sqrt{\pi}\exp\left(\frac{3+2\pi C_2}{4}\right)\sigma \approx 5.1\sigma & \text{(2D)}, \\ \frac{2}{3}\pi C_3\sigma \approx 3.2\sigma & \text{(3D)}. \end{cases} \tag{13}$$

Let $\tau^{\text{rebind}}_{\text{meso}}(k_a^{\text{meso}},h)$ and $\tau^{\text{rebind}}_{\text{micro}}(k_a)$ denote the average rebinding times—that is, the average time until two molecules react, given that they have just dissociated—on the mesoscopic and microscopic scale, respectively. Again, to simplify notation, we let $\tau^{\text{rebind},\rho}_{\text{meso}}(k_a,h) := \tau^{\text{rebind}}_{\text{meso}}(\rho^{(d)}(k_a,h),h)$. The rebinding times can be written in terms of the average binding times

$$\tau^{\text{rebind},\rho}_{\text{meso}}(k_a,h) = \tau^{\rho}_{\text{meso}}(k_a,h) - \tau^{\rho}_{\text{meso}}(\infty,h), \tag{14}$$

$$\tau^{\text{rebind}}_{\text{micro}}(k_a) = \tau_{\text{micro}}(k_a) - \tau_{\text{micro}}(\infty), \tag{15}$$

where, for simplicity of notation, $\tau^{\rho}_{\text{meso}}(k_a \to \infty,h)$ and $\tau_{\text{micro}}(k_a \to \infty)$ are denoted $\tau^{\rho}_{\text{meso}}(\infty,h)$ and $\tau_{\text{micro}}(\infty)$, respectively. That (14) and (15) hold can be realized by considering the following argument. Given a uniform initial distribution, $\tau_{\text{meso}}(\infty)$ is the time until the molecules are in the same voxel for the first time. By subtracting that time from the total binding time, we obtain the rebinding time. A similar argument holds for the microscopic case. We immediately see that because $\tau^{\rho}_{\text{meso}}(k_a,h) = \tau_{\text{micro}}(k_a)$ holds, the rebinding times will match if and only if $\tau^{\rho}_{\text{meso}}(\infty,h) = \tau_{\text{micro}}(\infty)$. This holds for $h = h^*_\infty$, and consequently,

$$\tau^{\text{rebind},\rho}_{\text{meso}}(k_a,h) > \tau^{\text{rebind}}_{\text{micro}}(k_a) \quad \text{for} \quad h > h^*_\infty, \tag{16}$$

$$\tau^{\text{rebind},\rho}_{\text{meso}}(k_a,h) = \tau^{\text{rebind}}_{\text{micro}}(k_a) \quad \text{for} \quad h = h^*_\infty, \tag{17}$$

$$\tau^{\text{rebind},\rho}_{\text{meso}}(k_a,h) < \tau^{\text{rebind}}_{\text{micro}}(k_a) \quad \text{for} \quad h < h^*_\infty. \tag{18}$$

As a mesoscopic dissociation event is a combination of microscopic dissociation and the diffusion required to get well mixed in a voxel, we require that $\tau^{\text{rebind}}_{\text{meso}} \geqslant \tau^{\text{rebind}}_{\text{micro}}$ hold. For $h < h^*_\infty$ we cannot match the mean binding time while satisfying $\tau^{\text{rebind}}_{\text{meso}} \geqslant \tau^{\text{rebind}}_{\text{micro}}$, and the accuracy of the sRDME consequently deteriorates with decreasing h. Thus, h^*_∞ is the finest spatial resolution attainable with the sRDME.

For a given $h > h^*_\infty$, we can compute the error in rebinding time as

$$\left|\tau^{\text{rebind},\rho}_{\text{meso}}(k_a,h) - \tau^{\text{rebind}}_{\text{micro}}(k_a)\right| = \left|\tau_{\text{meso}}(\infty,h) - \tau_{\text{micro}}(\infty)\right|, \tag{19}$$

where the right-hand side thus is a measure of how well resolved a system is. Details of the above theory are given in [17].

III. THE GENERALIZED REACTION-DIFFUSION MASTER EQUATION

In the sRDME, molecules react only when they occupy the same voxel. In this section we extend this approach by allowing molecules occupying neighboring voxels to react. To connect the sRDME to the microscopic Smoluchowski model we determined the rate at which molecules react when occupying the same voxel. For the gRDME we need to obtain the rates for molecules occupying the same voxel, but also the rates for molecules occupying neighboring voxels. In [16] and [17] we derive rates for the sRDME by matching the mean association times on the two scales. To uniquely determine both of the rates for the gRDME we need an additional constraint.

In Sec. III A we outline the algorithm, and in Sec. III B we derive mesoscopic parameters by trying to match certain statistics of the microscopic model to the corresponding statistics on the mesoscopic scale. In Sec. III C we determine the dissociation rate of a reversibly reacting pair of molecules, and in Sec. III D we collect the results and summarize the algorithm.

A. Generalized reactions

Consider a domain Ω discretized by a Cartesian mesh and a single reversible reaction $S_1 + S_2 \underset{k_d}{\overset{k_a}{\rightleftarrows}} S_3$. In the gRDME we allow reactions between molecules occupying neighboring voxels. Thus, if a molecule of species S_1 occupies the same voxel as a molecule of species S_2, they react with an intensity given by k_0. If the molecules instead occupy neighboring voxels they react with an intensity of k_1, where two voxels are neighbors if they share one side.

We can choose k_0 and k_1 freely, with the restriction that the total intensity should be constant. Call the total intensity

k_a^{meso}. Let d be the dimension. Then, since each voxel has $2d$ neighbors, k_0 and k_1 must satisfy

$$k_0 + 2dk_1 = k_a^{\text{meso}}. \tag{20}$$

Thus we can write

$$k_0 = (1 - 2dr)k_a^{\text{meso}}, \tag{21}$$

$$k_1 = rk_a^{\text{meso}}, \tag{22}$$

where $0 \leqslant r \leqslant 1/(2d)$.

Now assume that a molecule of species S_3 dissociates. We must determine where to place the two products S_1 and S_2. It may seem natural to place them in the same voxel with probability $1 - 2dr$ and in neighboring voxels with probability $2dr$. While this arguably would yield the most accurate results compared to microscopic simulations for a single reversible reaction, we show below that this approach is unsuitable in general.

First, consider the single irreversible dissociation given by

$$P \xrightarrow{k_{\text{deg}}} S_1 + S_2. \tag{23}$$

In this case the microscopic and mesoscopic rates will be the same; thus $k_d^{\text{meso}} = k_{\text{deg}}$, and the products are placed in the same voxel. Now consider that in addition to (23) we have the following reactions:

$$S_1 \xrightarrow{k^*} S_1^*, \tag{24}$$

$$S_1^* + S_2 \underset{k_d}{\overset{k_a}{\rightleftarrows}} S_3. \tag{25}$$

Again, (24) is an irreversible unimolecular reaction and thus the mesoscopic and microscopic rates are the same. Now, if k^* is large, the system (23)–(25) will be well approximated by

$$P \xrightarrow{k_{\text{deg}}} S_1^* + S_2 \underset{k_d}{\overset{k_a}{\rightleftarrows}} S_3. \tag{26}$$

Had we derived rates for reaction (25) assuming that dissociating molecules are placed in neighboring voxels with some probability, we can see that sequence (26) will be incorrectly simulated, as S_1 and S_2 are placed in the same voxel with probability 1 when P dissociates. Specifically, the rebinding dynamics of S_1^* and S_2 will be incorrect, as the rebinding time will depend on whether they were produced from a dissociating S_3 or a dissociating P.

To summarize:

(1) Reactive molecules occupying the same voxel react with intensity $(1 - 2dr)k_a^{\text{meso}}$.

(2) Reactive molecules in neighboring voxels react with intensity rk_a^{meso}.

(3) When a molecule dissociates, the products are placed in the same voxel with probability 1.

The parameters r and k_a^{meso} now have to be determined from the microscopic parameters k_a, σ, and D.

B. Reaction rates

Consider the reversible reaction $S_1 + S_2 \underset{k_d}{\overset{k_a}{\rightleftarrows}} S_3$. Assume that the initial state of the system is given by one molecule of species S_1 and one molecule of species S_2 in a square (2D) or a cubic (3D) domain Ω of width L with periodic boundary conditions. For simplicity, and without loss of generality, assume that the S_1 molecule is fixed at the origin while the S_2 molecule has a uniform initial distribution and a diffusion rate $D = D_1 + D_2$. On the microscopic scale the S_2 molecule moves by continuous Brownian motion. On the mesoscopic scale, Ω is subdivided into nonoverlapping squares or cubes of width h. The S_2 molecule thus jumps between voxels with a total intensity of $k_j = 2dD/h^2$ in dimension d. Let $\tau_{\text{meso,r}}(k_a^{\text{meso}},h)$ denote the average time until the molecules react on the mesoscopic scale in the gRDME.

For the sRDME, it was shown in [16] and [17] that by enforcing the constraint $\tau_{\text{meso}} = \tau_{\text{micro}}$ we obtain mesoscopic reaction rates as given by (10). In addition, it was shown that $\tau_{\text{meso}}^{\text{rebind}}$ approaches $\tau_{\text{micro}}^{\text{rebind}}$ from above as $h \to h_\infty^*$. Therefore it seems reasonable to require that with the gRDME we obtain an approximation of $\tau_{\text{micro}}^{\text{rebind}}$ that is equal to or better than the approximation we obtain with the sRDME. The first constraint is therefore that the mean binding time agrees between the mesoscopic and the microscopic scales,

$$\tau_{\text{meso,r}}\left(k_a^{\text{meso}},h\right) = \tau_{\text{micro}}(k_a), \tag{27}$$

and the second constraint is that, given (27), k_a^{meso} and r minimize the difference in the rebinding times at the mesoscopic vs microscopic scale; that is, we want to minimize

$$\left|\tau_{\text{meso,r}}^{\text{rebind}}\left(k_a^{\text{meso}},h\right) - \tau_{\text{micro}}^{\text{rebind}}(k_a)\right|, \tag{28}$$

under the assumption that (27) holds, where $\tau_{\text{meso,r}}$ is the average binding time (dependent on r and k_a^{meso}) and where $\tau_{\text{meso,r}}^{\text{rebind}}$ is the average rebinding time in the gRDME. Note that with (27) satisfied we have $\tau_{\text{meso,0}}(k_a^{\text{meso}},h) = \tau_{\text{meso}}(k_a^{\text{meso}},h)$ and $\tau_{\text{meso,0}}^{\text{rebind}}(k_a^{\text{meso}},h) = \tau_{\text{meso}}^{\text{rebind}}(k_a^{\text{meso}},h)$.

1. *Mean mesoscopic binding time*

Again, assume that we have species S_1 and S_2, with one molecule of each, and that the S_1 molecule is fixed. The S_2 molecule is initialized according to a uniform distribution and diffuses at diffusion rate D.

We start by deriving the mesoscopic mean binding time. To this end, let M_s^i denote the average number of diffusive jumps required for the S_2 molecule to reach a voxel at distance i from the S_1 molecule, where the distance between two voxels is defined to be the smallest number of discrete jumps required to move from one voxel to the other. Let the set of all voxels at a distance i from the S_1 molecule be denoted d_i (note that d_0 will then be a set of only one voxel; specifically, the voxel occupied by the S_1 molecule), let t_j denote the average time for a diffusive jump, and let τ_i denote the average time for the S_2 and the S_1 molecule to react, given that the S_2 molecule is occupying a voxel at distance i from the S_1 molecule. Thus, $t_j = h^2/(2dD)$, and

$$\tau_{\text{meso,r}}\left(k_a^{\text{meso}},h\right) = M_s^1 t_j + \tau_1. \tag{29}$$

The first term, $M_s^1 t_j$, represents the average time required for the S_2 molecule to reach d_1. The second term, τ_1, represents the remaining time until the molecules react, given that the S_2 molecule occupies a voxel in d_1.

a. Derivation of M_s^1. In this section we show that

$$M_s^1 = \begin{cases} \pi^{-1} N \ln N + (C_2 - 1)N + O(1) & \text{(2D)}, \\ (C_3 - 1)N + O(\sqrt{N}) & \text{(3D)}, \end{cases} \tag{30}$$

where C_2 and C_3 are defined in (12). Let M_i^j denote the average number of steps required to diffuse from d_i to d_j. We also show that

$$M_2^1 = \frac{N-2}{2d-1}. \tag{31}$$

To obtain (30) we first note that

$$M_s^1 = M_s^0 - M_1^0. \tag{32}$$

In [27] it is shown that

$$M_s^0 = \begin{cases} \pi^{-1} N \ln N + C_2 N + O(1) & \text{(2D)}, \\ C_3 N + O(\sqrt{N}) & \text{(3D)}. \end{cases} \tag{33}$$

Let M_0^0 be the average number of steps required to return to d_0, given that we start in d_0. The first jump of a molecule starting in d_0 always transfers the molecule to d_1, so we find that

$$M_1^0 = M_0^0 - 1. \tag{34}$$

We know that $M_0^0 = N$, shown in [26]. By combining (32), (33), and (34), we obtain (30).

To obtain (31) we note that we can write M_0^0 as

$$M_0^0 = 1 + \frac{1}{2d} + \frac{2d-1}{2d}\left(M_2^1 + M_1^0\right). \tag{35}$$

To see that the above equality holds, start by considering a molecule in d_0. The first jump transfers the molecule to d_1; the second jump transfers it back to the origin with a probability of $1/(2d)$ or to d_2 with a probability of $(2d-1)/(2d)$. The average number of steps required to reach d_0 from d_2 is given by the average number of steps to reach d_1 plus the average number of steps to reach d_0, given that the molecule starts in d_1. Now, solving (35) for M_2^1 yields (31).

b. Derivation of τ_1. To obtain $\tau_{\text{meso,r}}$ for $k_a < \infty$, it remains to determine τ_1. To that end, assume that the S_2 molecule occupies a voxel in d_1 and that the intensity with which the molecules react in d_1 is given by $1/(rk_a^{\text{meso}})$. Then, to maintain a total intensity of $1/k_a^{\text{meso}}$, the molecules must react with an intensity of $1/[(1-2dr)k_a^{\text{meso}}]$ in d_0. We require that $r \geqslant 0$ and that $0 \leqslant 1 - 2dr \leqslant 1$. To simplify the notation we let $1/(rk_a^{\text{meso}})$ be denoted by p_1 and $1/[(1-2dr)k_a^{\text{meso}}]$ by p_0.

Let t_e^0 and t_e^1 denote the average time until the next event fires, given that the S_2 molecule occupies a voxel in d_0 or d_1, respectively. Then $t_e^0 = 1/(p_0^{-1} + t_j^{-1})$ and $t_e^1 = 1/(p_1^{-1} + t_j^{-1})$.

By assumption, the S_2 molecule initially occupies a voxel in d_1. The next event can either be (1) a diffusive jump, with probability $p_1/(p_1 + t_j)$, or (2) a reaction event with probability $t_j/(p_1 + t_j)$.

Now assume that the next event is a diffusion event. Then (1.1) the molecule jumps to d_2 with probability $(2d-1)/2d$ or (1.2) the molecule jumps to d_0 with probability $1/(2d)$. Assume that the molecule jumps to d_0. Then the next event is (1.2.1) a reaction with probability $t_j/(p_0 + t_j)$ or (1.2.2) diffusion to d_1 with probability $p_0/(p_0 + t_j)$. Thus, if the molecule is in state (1.2), the time until the molecules react is given by

$$\tau_0 = \frac{t_j}{p_0 + t_j} t_e^0 + \frac{p_0}{p_0 + t_j}\left(t_e^0 + \tau_1\right) = t_e^0 + \frac{p_0}{p_0 + t_j}\tau_1. \tag{36}$$

Now instead assume that the molecule is in state (1.1). The molecules cannot react until the S_2 molecule reaches d_1, and thus the average time until the molecules react is given by

$$\tau_2 = M_2^1 t_j + \tau_1 = \frac{N-2}{2d-1} t_j + \tau_1, \tag{37}$$

where M_2^1 is given by (31). To summarize:

The S_2 molecule initially occupies a voxel in d_1, and the S_1 molecule is fixed in d_0.

(1) The S_2 molecule diffuses with probability $p_1/(p_1 + t_j)$.

(1.1) The S_2 molecule jumps to d_2 with probability $(2d-1)/(2d)$. The average remaining time until the S_1 and S_2 molecules react is given by τ_2.

(1.2) The S_2 molecule jumps to d_0 with probability $1/(2d)$.

(1.2.1) The S_1 and S_2 molecules react with probability $t_j/(p_0 + t_j)$.

(1.2.2) The S_2 molecule diffuses to d_1 with probability $p_0/(p_0 + t_j)$. The average remaining time until the S_1 and S_2 molecules react is given by τ_1.

(2) The S_1 and S_2 molecules react with probability $t_j/(p_1 + t_j)$.

Putting it all together, we obtain

$$\tau_1 = \frac{t_j}{p_1 + t_j} t_e^1 + \frac{p_1}{p_1 + t_j}\left(t_e^1 + \frac{1}{2d}\tau_0 + \frac{2d-1}{2d}\tau_2\right). \tag{38}$$

By inserting (36) and (37) into (38) and solving for τ_1 we obtain

$$\tau_1 = \frac{(N + 2d - 1)p_0 + (N + 2d - 2)t_j}{2d(p_0 + t_j) + p_1} p_1 \tag{39}$$

$$\approx \frac{p_0 + t_j}{p_0 + 2drt_j} \frac{N}{k_a^{\text{meso}}}, \tag{40}$$

after some cumbersome but straightforward algebra, where (40) follows by assuming $N \gg 1$.

c. Analytical expression for $\tau_{\text{meso,r}}$. Now, using (29), (30), and (40) we find that

$$\tau_{\text{meso,r}}\left(k_a^{\text{meso}}, h\right) \approx \begin{cases} [\pi^{-1} N \ln N + (C_2 - 1)N]t_j + \frac{p_0 + t_j}{p_0 + 4rt_j} \frac{N}{k_a^{\text{meso}}} & \text{(2D)}, \\ (C_3 - 1)Nt_j + \frac{p_0 + t_j}{p_0 + 6rt_j} \frac{N}{k_a^{\text{meso}}} & \text{(3D)}. \end{cases} \tag{41}$$

d. Lower limit on the voxel size. It is of interest to know the smallest voxel size h for which we can match the mesoscopic mean binding time, $\tau_{\text{meso,r}}$, with the microscopic mean binding time, τ_{micro}. In [16,17] this problem was solved in the case of the sRDME for a general reversible reaction $S_1 + S_2 \underset{k_d}{\overset{k_a}{\rightleftharpoons}} S_3$. Similar results in the case of the gRDME can be obtained for the case of an irreversible reaction with $k_a \to \infty$. As we see in Eqs. (74) and (75), the lower bound for $k_a \to \infty$ is in fact a fundamental lower bound for the gRDME.

We now let $h^*_{k_a,g}$ be the smallest voxel size for which we can choose reaction rates such that $\tau_{\text{meso,r}}(k_a^{\text{meso}}, h) = \tau_{\text{micro}}(k_a)$.

It is easy to see that $h^*_{k_a,g}$ exists; the average time until two molecules on the mesoscopic scale occupy the same or neighboring voxels diverges in two and three dimensions, thus there must exist a smallest mesh size for which the mesoscopic mean binding time can match the mean microscopic binding time. We do not have analytical results for τ_{micro} on a square or a cube, but given that $L \gg \sigma$ is satisfied, an excellent approximation is provided by

$$\tau_{\text{micro}}(k_a) = \begin{cases} \frac{1+\alpha F(\lambda)}{k_a} L^2 & \text{(2D)}, \\ \frac{L^3}{k_{\text{CK}}} & \text{(3D)}, \end{cases} \tag{42}$$

where

$$\begin{aligned} \lambda &= \pi^{\frac{1}{2}} \frac{\sigma}{L}, \\ \alpha &= \frac{k_a}{2\pi D}, \\ F(\lambda) &= \frac{\ln(1/\lambda)}{(1-\lambda^2)^2} - \frac{3-\lambda^2}{4(1-\lambda^2)} \end{aligned} \tag{43}$$

and where $k_{\text{CK}} = 4\pi\sigma D k_a/(4\pi\sigma D + k_a)$ is the classical mesoscopic reaction rate, valid for large volumes, derived by Collins and Kimball in [28]. The 2D expression was derived in [19], following the approach devised in [29].

Since molecules are allowed to react with molecules occupying neighboring voxels, we obtain

$$\tau_1 \to 0 \quad \text{for} \quad k_a \to \infty, \quad r > 0, \tag{44}$$

and thus

$$\tau_{\text{meso,r}} \to M_s^1 t_j \quad \text{for} \quad k_a \to \infty, \quad r > 0. \tag{45}$$

We know M_s^1 from (30), and we have $t_j = h^2/(2dD)$ by definition. We now obtain $h^*_{k_a,g}$ by solving

$$M_s^1 t_j = \tau_{\text{micro}}(\infty) \tag{46}$$

for h.

In three dimensions, (46) becomes

$$\frac{(C_3-1)L^3}{6Dh} = \frac{L^3}{4\pi\sigma D}, \tag{47}$$

since $M_s^1 \sim (C_3-1)N$ for $N \gg 1$, and $k_{\text{CK}} \to 4\pi\sigma D$ as $k_a \to \infty$. Solving (47) for h yields

$$h = \tfrac{2}{3}(C_3-1)\pi\sigma \approx 1.0815\sigma. \tag{48}$$

In two dimensions, (46) becomes

$$\frac{h^2}{4D}\left[\pi^{-1}\frac{L^2}{h^2}\ln\left(\frac{L^2}{h^2}\right) + (C_2-1)\frac{L^2}{h^2}\right] = \frac{L^2}{k_a} + \frac{F(\lambda)}{2\pi D}L^2, \tag{49}$$

and for $k_a \to \infty$, we have

$$\frac{L^2}{k_a} + \frac{F(\lambda)}{2\pi D}L^2 \to \frac{\ln\left(\pi^{-\frac{1}{2}}\frac{L}{\sigma}\right) - \frac{3}{4}}{2\pi D}L^2. \tag{50}$$

In (50) we used that $\lambda \approx 0$ for $L \gg \sigma$. Now (49) reduces to

$$\pi^{-1}\ln\left(\frac{L}{h}\right) + \frac{C_2-1}{2} = \pi^{-1}\ln\left(\pi^{-\frac{1}{2}}\frac{L}{\sigma}\right) - \frac{3}{4\pi}. \tag{51}$$

We can rewrite the equation above to get

$$\pi^{-1}\ln\left(\pi^{\frac{1}{2}}\frac{\sigma}{h}\right) = \frac{1-C_2}{2} - \frac{3}{4\pi}. \tag{52}$$

Solving for h yields

$$h = \sqrt{\pi}\exp\left(\frac{3+2\pi(C_2-1)}{4}\right)\sigma \approx 1.0599\sigma. \tag{53}$$

To summarize, we find that

$$h^*_{\infty,g} = \begin{cases} \sqrt{\pi}\exp\left(\frac{3+2\pi(C_2-1)}{4}\right)\sigma \approx 1.0599\sigma & \text{(2D)}, \\ \frac{2}{3}(C_3-1)\pi\sigma \approx 1.0815\sigma & \text{(3D)}. \end{cases} \tag{54}$$

2. Mean mesoscopic rebinding time

To satisfy the second constraint, (28), we need both the microscopic and the mesoscopic mean rebinding times. The microscopic rebinding time is derived in [17], as

$$\tau^{\text{rebind}}_{\text{micro}} = \frac{L^d}{k_a}. \tag{55}$$

The mesoscopic rebinding time is simply given by

$$\tau^{\text{rebind}}_{\text{meso}} = \tau_0, \tag{56}$$

as τ_0 by definition is the time until an S_1 and an S_1 molecule react, given that they start in the same voxel. We have already derived τ_0 in terms of τ_1 in (36), and we thus obtain

$$\tau^{\text{rebind}}_{\text{meso,r}} \approx t_e^0 + \frac{p_0}{p_0 + 2drt_j}\frac{N}{k_a^{\text{meso}}} \tag{57}$$

immediately from (39) and (40).

3. Solving for r and k_a^{meso}

We now want r and k_a^{meso} to satisfy constraints (27) and (28). It will prove useful to divide the problem into two cases.

$$\text{Case 1:} \quad h \geqslant h^*_\infty. \tag{58}$$

$$\text{Case 2:} \quad h^*_\infty > h \geqslant h^*_{\infty,g}. \tag{59}$$

It turns out that in case 1 we get $r = 0$, effectively reducing the generalized algorithm to the standard algorithm.

a. Case 1. We assume that r and k_a^{meso} have been chosen to satisfy the first constraint, (27), and then show that for $h \geqslant h^*_\infty$ we have

$$\tau^{\text{rebind}}_{\text{meso,r}}\left(k_a^{\text{meso}}, h\right) \gtrapprox \tau^{\text{rebind},\rho}_{\text{meso}}(k_a, h). \tag{60}$$

Since $\tau^{\text{rebind},\rho}_{\text{meso}}(k_a,h) \geqslant \tau^{\text{rebind}}_{\text{micro}}(k_a)$, it immediately follows that for $h \geqslant h^*_\infty$, the gRDME and the sRDME agree.

We first note that we already know that

$$\tau_{\text{meso}} = M_s^0 t_j + \tau_0, \tag{61}$$

$$\tau_{\text{meso,r}} = M_s^1 t_j + \tau_1^g, \tag{62}$$

where τ_i, as previously defined, is the average time until the molecules react, given that the S_2 molecule is in d_i. The superscript g indicates that it is the average time in the case of the gRDME, and omission of the superscript indicates that it is the average time in the case of the sRDME.

We have assumed that (27) is satisfied, and consequently,

$$0 = \tau_{\text{meso}} - \tau_{\text{meso,r}} = \left(M_s^0 - M_s^1\right)t_j + \left(\tau_0 - \tau_1^g\right) = Nt_j + \left(\tau_0 - \tau_1^g\right), \tag{63}$$

where the second equality follows from (30) and (33). We know that $\tau_{\text{meso}}^{\text{rebind}} = \tau_0$, so we get

$$\tau_{\text{meso}}^{\text{rebind}} = \tau_1^g - Nt_j. \tag{64}$$

Thus

$$\tau_{\text{meso,r}}^{\text{rebind}} \geqslant \tau_{\text{meso}}^{\text{rebind}} \tag{65}$$

$$\iff \tau_0^g \geqslant \tau_1^g - Nt_j \tag{66}$$

$$\iff \tau_1^g - \tau_0^g \leqslant Nt_j. \tag{67}$$

We have already shown that

$$\tau_0^g = t_e^0 + \frac{p_0}{p_0 + t_j}\tau_1^g > \frac{p_0}{p_0 + t_j}\tau_1^g, \tag{68}$$

$$\tau_1^g \approx \frac{p_0 + t_j}{p_0 + 2drt_j}\frac{N}{k_a^{\text{meso}}}. \tag{69}$$

Now (67) becomes

$$\frac{p_0 + t_j}{p_0 + 2drt_j}\frac{N}{k_a^{\text{meso}}} - \frac{p_0}{p_0 + t_j}\frac{p_0 + t_j}{p_0 + 2drt_j}\frac{N}{k_a^{\text{meso}}} \leqslant Nt_j \tag{70}$$

$$\iff \frac{1}{p_0 + 2drt_j}\frac{1}{k_a^{\text{meso}}} \leqslant 1. \tag{71}$$

By definition, $p_0 = 1/(1-2dr)k_a^{\text{meso}}$, so (71) becomes

$$\frac{1}{\frac{1}{(1-2dr)k_a^{\text{meso}}} + 2drt_j}\frac{1}{k_a^{\text{meso}}} \leqslant 1 \tag{72}$$

$$\iff 1 \leqslant (1-2dr)^{-1} + 2drt_j k_a^{\text{meso}}. \tag{73}$$

Since $1 - 2dr \leqslant 1$, we have $(1-2dr)^{-1} \geqslant 1$, and $2drt_j k_a^{\text{meso}} \geqslant 0$ so (73) is satisfied for all r and k_a^{meso}. Thus (65) holds for all r and k_a^{meso}.

What remains is to determine r and k_a^{meso} for $h < h_{\infty}^*$.

b. Case 2. We proceed in two steps. First, we show that for $h = h_{\infty,g}^*$ with $\tau_1 \gg t_e^0$ we have

$$\tau_{\text{meso,r}}\left(k_a^{\text{meso}}, h\right) \approx \tau_{\text{micro}}(k_a), \tag{74}$$

$$\tau_{\text{meso,r}}^{\text{rebind}}\left(k_a^{\text{meso}}, h\right) \approx \tau_{\text{micro}}^{\text{rebind}}(k_a) \tag{75}$$

for $k_a^{\text{meso}} = k_a/h^d$ and $1 - 2dr = 0$, and for $h < h_{\infty,g}^*$

$$\tau_{\text{meso,r}}^{\text{rebind}}\left(k_a^{\text{meso}}, h\right) \lessapprox \tau_{\text{micro}}^{\text{rebind}}(k_a). \tag{76}$$

Note that we have already shown that we can satisfy (27) at least down to $h = h_{\infty,g}^*$. The assumption $\tau_1 \gg t_e^0$ means, in words, that the *average* time until two molecules react, given that they are one voxel apart, is much longer than the average time until the first event, given that they occupy the same voxel. Unless the microscopic reaction rate is very high, this should be a reasonable assumption for most systems. The necessity of this assumption is realized by considering two molecules in the same voxel. Now, if the average microscopic rebinding time is shorter than the average time until the first diffusion event on the mesoscopic scale, we could not hope to find mesoscopic rates that will yield a match between the mesoscopic rebinding time and the microscopic rebinding time.

To show that (74) and (75) hold, we first note that we already know that

$$\tau_{\text{meso,r}}\left(k_a^{\text{meso}}, h\right) = M_s^1 t_j + \tau_1, \tag{77}$$

and from assuming $h = h_{\infty,g}^*$, it follows that

$$M_s^1 t_j = \tau_{\text{micro}}(\infty), \tag{78}$$

and thus

$$\tau_{\text{meso,r}}\left(k_a^{\text{meso}}, h_{\infty,g}^*\right) = \tau_{\text{micro}}(\infty) + \tau_1. \tag{79}$$

Equations (39) and (40) yield, for $1 - 2dr = 0$ and $k_a^{\text{meso}} = k_a/h^d$,

$$\tau_1 = \frac{N}{k_a^{\text{meso}}} = \frac{Nh^d}{k_a} = \frac{L^d}{k_a} = \tau_{\text{micro}}^{\text{rebind}}(k_a). \tag{80}$$

We now have

$$\tau_{\text{meso,r}}\left(\frac{k_a}{h^d}, h_{\infty,g}^*\right) = \tau_{\text{micro}}(\infty) + \tau_{\text{micro}}^{\text{rebind}}(k_a) = \tau_{\text{micro}}(k_a), \tag{81}$$

and thus (74) holds. Since we have assumed that $\tau_1 \gg t_e^0$ and $1 - 2dr = 0$, we get

$$\tau_{\text{meso,r}}^{\text{rebind}}\left(\frac{k_a}{h^d}, h_{\infty,g}^*\right) = \tau_0 \approx \tau_1 = \tau_{\text{micro}}^{\text{rebind}}(k_a), \tag{82}$$

and we have shown that (75) holds.

It remains to show (76). To this end, we simply note that

$$\tau_{\text{micro}}(k_a) = \tau_{\text{meso,r}} = M_s^1 t_j + \tau_1 > \tau_{\text{micro}}(\infty) + \tau_1, \tag{83}$$

since $M_s^1 t_j > \tau_{\text{micro}}(\infty)$ for $h < h_{\infty,g}^*$. Thus

$$\tau_{\text{micro}}^{\text{rebind}} = \tau_{\text{micro}}(k_a) - \tau_{\text{micro}}(\infty) > \tau_1 \approx \tau_0 = \tau_{\text{meso,r}}^{\text{rebind}}, \tag{84}$$

and (76) follows.

Second, we show that for $h_{\infty,g}^* < h < h_{\infty}^*$, still assuming that $\tau_1 \gg t_e^0$, we have

$$\tau_{\text{meso,r}}\left(k_a^{\text{meso}}, h\right) \approx \tau_{\text{micro}}(k_a), \tag{85}$$

$$\tau_{\text{meso,r}}^{\text{rebind}}\left(k_a^{\text{meso}}, h\right) \approx \tau_{\text{micro}}^{\text{rebind}}(k_a) \tag{86}$$

for

$$k_a^{\text{meso}} = \left(\frac{t_j Q^2 + k_a/h^d}{t_j Q^2 + Q k_a/h^d}\right)\frac{k_a}{h^d}, \tag{87}$$

$$r = \frac{DQ(Q-1)}{2dDQ^2 + k_a/h^{d-2}}, \tag{88}$$

where

$$Q = \frac{Nt_j}{\tau_{\text{micro}}(\infty) - \tau_{\text{meso,r}}(\infty)} = \begin{cases} \left[\frac{2}{\pi}\ln\left(\frac{h}{h^*_{\infty,g}}\right)\right]^{-1} & \text{(2D)}, \\ \left[(C_3-1)\left(\frac{h}{h^*_{\infty,g}}-1\right)\right]^{-1} & \text{(3D)}. \end{cases} \tag{89}$$

We show this by first noting that we already know that

$$\tau_{\text{meso,r}}\left(k_a^{\text{meso}},h\right) = M_s^1 t_j + \tau_1, \tag{90}$$

$$\tau_{\text{micro}}^{\text{rebind}}(k_a) = \tau_{\text{micro}}(k_a) - \tau_{\text{micro}}(\infty) = \frac{Nh^d}{k_a}, \tag{91}$$

$$\tau_{\text{meso,r}}^{\text{rebind}}\left(k_a^{\text{meso}},h\right) = \tau_0 \approx \frac{p_0}{p_0 + 2drt_j}\frac{N}{k_a^{\text{meso}}}. \tag{92}$$

Consequently, we satisfy (85) if

$$M_s^1 t_j + \tau_1 = \tau_{\text{micro}}(k_a), \tag{93}$$

which, by (39) and (40), approximately holds if

$$\frac{p_0 + t_j}{p_0 + 2drt_j}\frac{N}{k_a^{\text{meso}}} = \tau_{\text{micro}}(k_a) - M_s^1 t_j. \tag{94}$$

To satisfy (86), we must, by (91) and (92), satisfy

$$\frac{p_0}{p_0 + 2drt_j}\frac{N}{k_a^{\text{meso}}} = \tau_{\text{micro}}^{\text{rebind}}(k_a). \tag{95}$$

Subtracting both the right-hand and the left-hand side of (95) from (94), we obtain

$$\frac{t_j}{p_0 + 2drt_j}\frac{N}{k_a^{\text{meso}}} = \tau_{\text{micro}}(k_a) - M_s^1 t_j - \tau_{\text{micro}}^{\text{rebind}}(k_a). \tag{96}$$

By definition, $p_0 = 1/(1-2dr)k_a^{\text{meso}}$ and $t_j = h^2/(2dD)$, so (96) yields, after some straightforward algebra,

$$k_a^{\text{meso}} = \left(\frac{(1-2dr)Nt_j}{\tau_{\text{micro}}(k_a) - M_s^1 t_j - \tau_{\text{micro}}^{\text{rebind}}(k_a)} - 1\right)\frac{D}{rh^2(1-2dr)}. \tag{97}$$

Since $\tau_{\text{meso,r}}(\infty) = M_s^1 t_j$ and $\tau_{\text{micro}}^{\text{rebind}}(k_a) = \tau_{\text{micro}}(k_a) - \tau_{\text{micro}}(\infty)$, (97) becomes

$$k_a^{\text{meso}} = \frac{D}{rh^2}\left(\frac{Nt_j}{\tau_{\text{micro}}(\infty) - \tau_{\text{meso,r}}(\infty)} - \frac{1}{1-2dr}\right) \tag{98}$$

$$= \frac{D}{rh^2}\left(Q - \frac{1}{1-2dr}\right). \tag{99}$$

With k_a^{meso} as in (99), we want to find r such that (95) is satisfied. Since $\tau_{\text{micro}}^{\text{rebind}} = L^d/k_a = Nh^d/k_a$, we obtain

$$\frac{p_0}{p_0 + 2drt_j}\frac{N}{k_a^{\text{meso}}} = \frac{Nh^d}{k_a} \tag{100}$$

$$\iff \frac{1}{1_2drt_j p_0^{-1}}\frac{1}{k_a^{\text{meso}}} = \frac{h^d}{k_a} \tag{101}$$

$$\iff \left(1 + 2drt_j p_0^{-1}\right)k_a^{\text{meso}} = \frac{k_a}{h^d}. \tag{102}$$

Since $t_j = h^2/2dD$ and $p_0 = 1/(1-2dr)k_a$, (102) becomes

$$\frac{rh^2}{D}(1-2dr)\left(k_a^{\text{meso}}\right)^2 + k_a^{\text{meso}} = \frac{k_a}{h^d}. \tag{103}$$

We expand the first term on the left-hand side to get

$$\frac{rh^2}{D}(1-2dr)\left(k_a^{\text{meso}}\right)^2 = \frac{D}{rh^2}\left[(1-2dr)Q^2 - 2Q + \frac{1}{1-2dr}\right]. \tag{104}$$

Thus

$$\frac{rh^2}{D}(1-2dr)\left(k_a^{\text{meso}}\right)^2 + k_a^{\text{meso}} = \frac{D}{rh^2}[(1-2dr)Q^2 - Q], \tag{105}$$

and (103) becomes

$$\frac{D}{rh^2}[(1-2dr)Q^2 - Q] = \frac{k_a}{h^d}, \tag{106}$$

yielding

$$r = \frac{DQ(Q-1)}{2dDQ^2 + \frac{k_a}{h^d}}. \tag{107}$$

Inserting r above into (99) yields (87).

It remains to show that $k_a^{\text{meso}} > 0$ and $0 < r < 1/(2d)$ hold for k_a^{meso} and r given by (87) and (88). We first show that $Q > 1$, from which $r > 0$ follows. Thus we should show that

$$Q = \frac{Nt_j}{\tau_{\text{micro}}(\infty) - \tau_{\text{meso,r}}(\infty)} > 1 \tag{108}$$

holds. We start by showing that (108) holds in three dimensions. By (30),

$$\tau_{\text{meso,r}}(\infty,h) \approx (C_3-1)Nt_j = (C_3-1)\frac{L^3}{h^3}\frac{h^2}{2dD} \tag{109}$$

for $N \gg 1$. We have already shown that

$$\tau_{\text{micro}}(\infty) = \tau_{\text{meso,r}}(\infty,h^*_{\infty,g}) = (C_3-1)\frac{L^3}{(h^*_{\infty,g})^3}t_j, \tag{110}$$

so (108) becomes

$$Q = \frac{\frac{L^3}{h^3}\frac{h^2}{2dD}}{(C_3-1)\frac{L^3}{(h^*_{\infty,g})^3}\frac{(h^*_{\infty,g})^2}{2dD} - (C_3-1)\frac{L^3}{h^3}\frac{h^2}{2dD}} = \frac{\frac{1}{h}}{(C_3-1)\left(\frac{1}{h^*_{\infty,g}} - \frac{1}{h}\right)} > 1 \tag{111}$$

$$\iff (C_3-1)\left(\frac{h}{h^*_{\infty,g}} - 1\right) < 1. \tag{112}$$

Since $h^*_\infty/h^*_{\infty,g} = C_3/(C_3-1)$, and by assumption, $h < h^*_\infty$, we obtain

$$(C_3-1)\left(\frac{h}{h^*_{\infty,g}} - 1\right) < (C_3-1)\left(\frac{C_3}{C_3-1} - 1\right) = 1. \tag{113}$$

Thus $Q > 1$, and as a consequence, $r > 0$. In two dimensions we have

$$\tau_{\mathrm{meso,r}}(\infty,h) = [\pi^{-1} N \ln N + (C_2 - 1)N]t_j \tag{114}$$

$$= \left[\pi^{-1}\frac{L^2}{h^2}\ln\frac{L^2}{h^2} + (C_2-1)\frac{L^2}{h^2}\right]\frac{h^2}{2dD} \tag{115}$$

$$= \pi^{-1}\frac{L^2}{2dD}\ln\frac{L^2}{h^2} + (C_2-1)\frac{L^2}{2dD}. \tag{116}$$

In two dimensions, similarly to the 3D case, we have $\tau_{\mathrm{micro}}(\infty) = \tau_{\mathrm{meso,r}}(\infty, h^*_{\infty,g})$. Thus

$$Q = \frac{\frac{L^2}{h^2}\frac{h^2}{2dD}}{\left[\pi^{-1}\frac{L^2}{2dD}\ln\frac{L^2}{(h^*_{\infty,g})^2} + (C_2-1)\frac{L^2}{2dD}\right] - \left[\pi^{-1}\frac{L^2}{2dD}\ln\frac{L^2}{h^2} + (C_2-1)\frac{L^2}{2dD}\right]} \tag{117}$$

$$= \frac{1}{2\pi^{-1}\left(\ln\frac{L}{h^*_{\infty,g}} - \ln\frac{L}{h}\right)} = \frac{1}{2\pi^{-1}\ln\frac{h}{h^*_{\infty,g}}}. \tag{118}$$

Since, by assumption,

$$1 < \frac{h}{h^*_{\infty,g}} < \frac{h^*_{\infty}}{h^*_{\infty,g}} \tag{119}$$

and

$$\frac{h^*_{\infty}}{h^*_{\infty,g}} = \exp\left[\frac{3+2\pi C_2}{4} - \frac{3+2\pi(C_2-1)}{4}\right] = \exp\left(\frac{\pi}{2}\right), \tag{120}$$

we obtain

$$Q = \frac{1}{2\pi^{-1}\ln\frac{h}{h^*_{\infty,g}}} > \frac{1}{2\pi^{-1}\ln\left(\exp\frac{\pi}{2}\right)} = 1. \tag{121}$$

Thus $Q > 1$ holds in both two and three dimensions, and we have $r > 0$. Note that with $Q > 1$, $k_a^{\mathrm{meso}} > 0$ follows immediately. It remains to show that $r < 1/(2d)$. To this end, we simply note that

$$r = \frac{DQ^2 - DQ}{2dDQ^2 + \frac{k_a}{h^{d-2}}} = \left(\frac{DQ^2 - DQ}{DQ^2 + \frac{k_a}{2dh^{d-2}}}\right)\frac{1}{2d}, \tag{122}$$

where

$$\frac{DQ^2 - DQ}{DQ^2 + \frac{k_a}{2dh^{d-2}}} < 1 \tag{123}$$

holds, since $Q > 1$. Thus $0 < r < 1/(2d)$ and $k_a^{\mathrm{meso}} > 0$ for $h^*_{\infty,g} < h < h^*_{\infty}$.

C. Dissociation rates

Consider the same setup as before, with one S_1 molecule and one S_2 molecule reacting reversibly according to $S_1 + S_2 \underset{k_d}{\overset{k_a}{\rightleftarrows}} S_3$. Above we have determined how to choose the mesoscopic association rates, so what remains is to determine the dissociation rate. This can be done completely analogously to the case of the sRDME. We thus follow the approach in [17] and conclude that we must have

$$\frac{\left(k_d^{\mathrm{meso}}\right)^{-1}}{\tau_{\mathrm{meso,r}}^{\mathrm{rebind}} + \left(k_d^{\mathrm{meso}}\right)^{-1}} = \frac{k_d^{-1}}{\tau_{\mathrm{micro}}^{\mathrm{rebind}} + k_d^{-1}} \tag{124}$$

to obtain a steady state on the mesoscopic scale that matches the steady state of the microscopic scale. Thus it follows immediately that for $h^*_{\infty,g} \leqslant h \leqslant h^*_{\infty}$, we should have

$$k_d^{\mathrm{meso}} = k_d, \tag{125}$$

because $\tau_{\mathrm{meso,r}}^{\mathrm{rebind}}(k_a^{\mathrm{meso}}, h) = \tau_{\mathrm{micro}}^{\mathrm{rebind}}(k_a)$ holds.

D. Summary of the algorithm

Assume that we have a cubic (3D) or square (2D) domain of width L, discretized by a Cartesian mesh with voxels of width h. Consider a reversible reaction $S_1 + S_2 \underset{k_d}{\overset{k_a}{\rightleftarrows}} S_3$, where k_a and k_d are the microscopic reaction rates. Let $D = D_1 + D_2$, where D_1 and D_2 are the diffusion rates of species S_1 and S_2, respectively. Let $\sigma = \sigma_1 + \sigma_2$ be the reaction radius of an S_1 and an S_2 molecule.

The critical mesh sizes are given by

$$h^*_{\infty} \approx \begin{cases} 5.1\sigma & \text{(2D)}, \\ 3.2\sigma & \text{(3D)} \end{cases} \tag{126}$$

for the sRDME, and the critical mesh sizes for the gRDME are given by

$$h^*_{\infty,g} \approx \begin{cases} 1.06\sigma & \text{(2D)}, \\ 1.08\sigma & \text{(3D)}. \end{cases} \tag{127}$$

We now wish to simulate this system on the mesoscopic scale with the gRDME. The results of this section can be summarized as follows:

(1) For $h \geqslant h^*_{\infty}$: The gRDME reduces to the sRDME. Thus $r = 0$ and $k_a^{\mathrm{meso}} = \rho^{(d)}(k_a, h)$. Molecules react only when occupying the same voxel. The dissociation rate is given by $k_d^{\mathrm{meso}} = h^d k_d k_a^{\mathrm{meso}}/k_a$, as shown in [17].

(2) For $h^*_{\infty,g} < h < h^*_{\infty}$: We match both the mean binding time and the mean rebinding time of the S_1 and S_2 molecules by choosing r and k_a^{meso} as in (87) and (88). Now molecules react with an intensity of rk_a^{meso} when occupying neighboring voxels and with an intensity of $(1 - 2dr)k_a^{\mathrm{meso}}$ when occupying the same voxel. The dissociation rate is simply given by $k_d^{\mathrm{meso}} = k_d$.

(3) For $h < h^*_{\infty,g}$ we can no longer match the mean rebinding time, and the accuracy deteriorates with decreasing h.

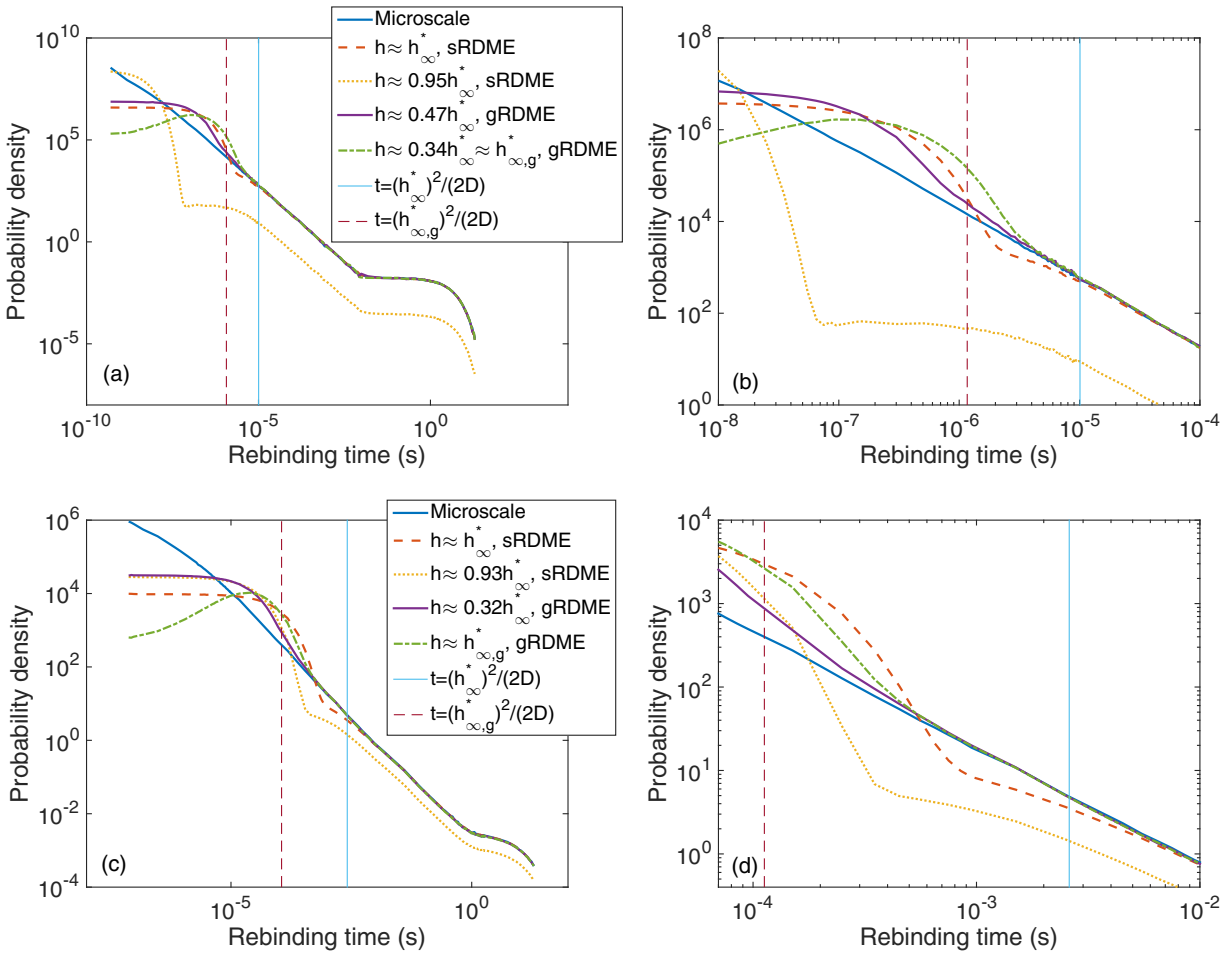

FIG. 1. (a, b) Rebinding-time distributions in three dimensions. For the sRDME we have a good match between the microscopic and the mesoscopic simulations for $h \approx h^*_\infty$, while the average rebinding time is underestimated for finer meshes. For the gRDME we see that the microscopic and mesoscopic distributions agree well for $h^*_{\infty,g} < h < h^*_\infty$ down to spatial resolution almost of the order of the size of the molecules, or a temporal resolution of approximately $(h^*_{\infty,g})^2/(2D)$. (c, d) Rebinding-time distributions in two dimensions. The conclusions are the same as for the 3D case. Parameters in (a) and (b) are given by $\sigma = 2 \times 10^{-9}$ m, $D = 2 \times 10^{-12}$ m^2 s^{-1}, $L = 5.145 \times 10^{-7}$ m, and $k_a = 10^{-18}$ m^3 s^{-1}. Parameters in (c) and (d) are given by $\sigma = 2 \times 10^{-9}$ m^2 s^{-1}, $D = 2 \times 10^{-14}$ m^2 s^{-1}, $L = 5.2 \times 10^{-7}$ m, and $k_a = 10^{-12}$m^2 s^{-1}.

IV. NUMERICAL RESULTS

A. Rebinding-time distributions

Consider a system of two species, S_1 and S_2, with one molecule of each. The S_1 molecule is fixed at the origin, while the S_2 molecule diffuses freely in space. In [17] it was shown that the sRDME matched the microscopic rebinding-time distribution for a reversibly reacting pair down to $t^* \sim (h^*_\infty)^2/(2D)$. For $t < t^*$, the behavior is inevitably going to be different, as the accuracy of the sRDME is inherently limited by the spatial resolution.

With the gRDME, we can match both the average binding times and the average rebinding times for $h^*_\infty \geqslant h \geqslant h^*_{\infty,g}$, and thus we would hope that also the error in distribution will be small at time scales of $(h^*_{\infty,g})^2/(2D) < t < (h^*_\infty)^2/(2D)$.

In Fig. 1 we compare the microscopic rebinding-time distribution (obtained using the microscopic algorithm described in [22]) to the rebinding-time distribution for the gRDME. As we can see, there is a good match down to a spatial resolution of approximately σ. For the finest meshes, the behavior at really short time scales is incorrect due to dissociating particles starting in the same voxel but not reacting until they are in neighboring voxels. This introduces an error of the order of the voxel size, which will be of the order of the size of the molecules.

B. Convergence of the generalized RDME

The dynamics of some systems is resolved only at a fine spatial resolution. In particular, it has been shown that fast rebinding events can affect, e.g., the response time of a MAPK pathway [6]. We consider the system

$$\begin{cases} S_1 \xrightarrow{k_d} S_{11} + S_{12} \xrightarrow{k_a} S_2, \\ S_2 \xrightarrow{k_d} S_{21} + S_{22} \xrightarrow{k_a} S_3, \end{cases} \tag{128}$$

which has a behavior similar to that of the MAPK pathway of [6]. Due to the possibility of fast rebinding events, the long-term dynamics of the system is affected by spatial correlations between newly produced molecules.

We start with an initial population of 100 S_1 molecules, with none of the other species present. The system is simulated for 2 s, during which we sample the state of the system at

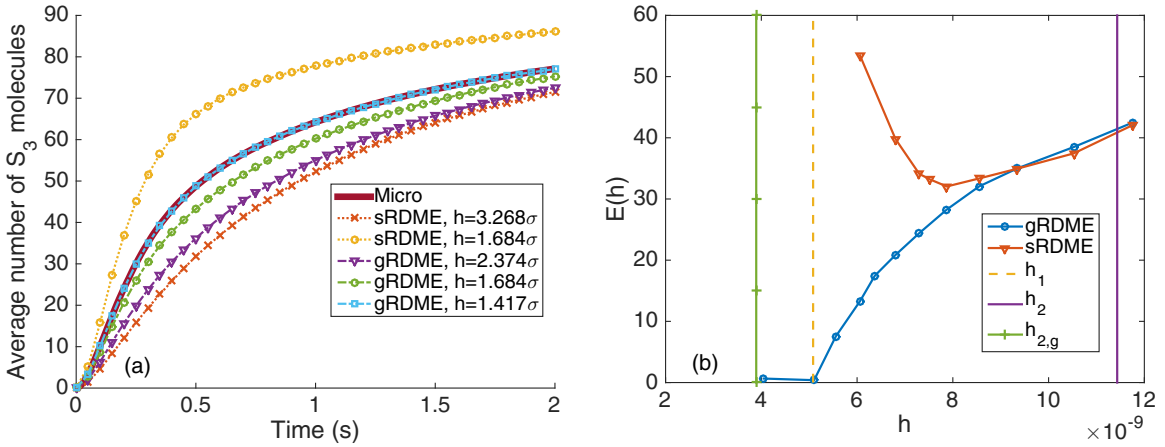

FIG. 2. (a) Average number of S_3 molecules as a function of time. As we can see, for a larger value of the voxel size h, we underestimate the number of S_3 molecules. For a very fine mesh, the number of S_3 molecules is overestimated with the sRDME. Somewhere in between we may obtain a good approximation compared to the microscopic results also with the sRDME, but then the concentration of other species in the system will be incorrect. For simulations with the generalized algorithm, the average number of S_3 molecules is underestimated for coarse meshes, but as we refine the mesh, the dynamics approaches that of the microscopic simulations. (b) The total error, as defined in (129), decreases to a mesh size of h_1 for the gRDME, while the error for the sRDME first decreases slightly but then increases as we refine the mesh further. We obtain an almost-perfect match between the microscopic simulations and the gRDME as h approaches h_1 and all the way down to $h_{2,g}$. The average on the microscopic scale is based on 2000 trajectories, giving 95% confidence intervals of width less than 0.2% of the mean for most time points, and the mesoscopic results are based on approximately 500 trajectories, giving 95% confidence intervals of width less than 1.0% of the mean for most time points.

201 evenly distributed points between $t = 0$ and $t = 2$. We simulate the system with both the sRDME and the gRDME, for different voxel sizes. Let $\mathcal{S} = \{S_1, S_{11}, S_{12}, S_2, S_{21}, S_{22}, S_3\}$. We define the error, $E(h)$, to be

$$E(h) = \frac{1}{201} \sum_{i=1}^{201} \sum_{S \in \mathcal{S}} \left| [S]_{h,i}^{\text{meso}} - [S]_i^{\text{micro}} \right|, \tag{129}$$

where $[S]_i^{\text{micro}}$ is the average population of S at time t_i, obtained with the microscopic algorithm from [22], and where $[S]_{h,i}^{\text{meso}}$ denotes the average population of S at time t_i obtained at the mesoscopic scale with voxel size h.

After a dissociation of either an S_1 or an S_2 molecule from (128), the products can rebind quickly to produce an S_2 or S_3 molecule, respectively. On the microscopic scale, the products are in contact after a dissociation event, and thus the spatial correlation will be significant. At the mesoscopic scale, the products are placed in the same voxel after a dissociation. If the voxel size is large compared to the size of the molecules, the spatial correlation will be less than on the microscale. Thus, to simulate (128) accurately, we would expect a fine-mesh resolution to be required.

Let σ_i be the reaction radius of molecule S_i and σ_{ij} the reaction radius of molecule S_{ij}. The parameters of the model are given by

$$\begin{cases} k_d = 10\ \text{s}^{-1}, \\ k_a = 10^{-19}\ \text{m}^3\ \text{s}^{-1} \end{cases} \qquad \begin{cases} \sigma_1 = 10^{-9}\ \text{m}, \\ \sigma_{11} = \sigma_{12} = 0.8 \times 10^{-9}\ \text{m}, \\ \sigma_2 = 2 \times 10^{-9}\ \text{m}, \\ \sigma_{21} = \sigma_{22} = 1.8 \times 10^{-9}\ \text{m}, \\ \sigma_3 = 2.5 \times 10^{-9}\ \text{m}. \end{cases} \tag{130}$$

For simplicity, we let all species have the same diffusion rate, $D = 10^{-12}\text{m}^2\ \text{s}^{-1}$. The S_1 molecules are initialized uniformly in a cube of volume 10^{-18} m.

There is a critical lower bound on the mesh size associated with each of the system's bimolecular reaction events:

$$\begin{cases} h_1 := h_\infty^*(\sigma_{11} + \sigma_{12}) \approx 5.0815 \times 10^{-9}, \\ h_2 := h_\infty^*(\sigma_{21} + \sigma_{22}) \approx 1.1433 \times 10^{-8}. \end{cases} \tag{131}$$

We know that for $h > h_\infty^*$, we are unable to match either the mesoscopic mean association time or the mesoscopic mean rebinding time to the corresponding microscopic quantities. Thus, for $h > \max\{h_1, h_2\}$, we will overestimate the rebinding time for both reactions and, consequently, underestimate the average S_3 concentration.

For $h_2 > h > h_1$ the dynamics is less obvious; we are underestimating the average rebinding time for the first reaction but overestimating the average rebinding time for the second. As shown in Fig. 2(b), the positive and negative errors partly cancel out in this regime. At first the error decreases with decreasing h, but as we approach h_1, it starts to increase again. The behavior of the sRDME is hard to predict, and *a priori* we cannot be sure that a particular choice of h is suitable.

In contrast, we see that the gRDME has a more predictable behavior, converging with decreasing h and yielding an almost-perfect match for $h < h_1$. The difference in behavior is due to the gRDME's matching the average rebinding time also for $h < h_\infty^*$, all the way down to $h_{2,g} := h_{\infty,g}^*(\sigma_{21} + \sigma_{22}) \approx 3.8934 \times 10^{-9}$.

At the finest mesh sizes a diffusion event will move a particle a distance of the order of the radius of the molecules. Thus, for a dilute system such as the above, it is noteworthy that an efficient microscopic method taking advantage of the large distances between molecules will be significantly faster than

the gRDME. For the problem above, the algorithm in [22] is more than an order of magnitude faster than the gRDME at the finest mesh sizes (one realization on the microscopic scale took around 8 s, while a simulation with the gRDME at the finest mesh size took around 150 s; note that both implementations were crude and not optimized). However, in the case of a less dilute system, we expect the gRDME to be more competitive. The execution time on the microscopic scale increases almost quadratically with the number of molecules but linearly with the number of molecules on the mesoscopic scale. A possible application of the gRDME is in hybrid methods, where part of the system can be simulated at the coarser sRDME scale, and only some parts of the system at the most fine-grained and expensive gRDME scale.

V. SUMMARY

For the sRDME there is a lower bound on the mesh size, h^*_∞, below which the accuracy deteriorates. For $h > h^*_\infty$ we match the mean binding time of two molecules with the mesoscopic reaction rate given by $\rho^{(d)}(k_a,h)$. For $h = h^*_\infty$ we match both the mean binding time and the mean rebinding time of the two molecules.

Some systems display fine-grained dynamics, requiring a fine spatial resolution to be simulated at the mesoscopic scale. By generalizing the sRDME to allow reactions between molecules in neighboring voxels, we obtain a lower bound on the mesh size given by $h^*_{\infty,g}$, where $h^*_{\infty,g}$ is of the order of the reaction radius of a pair of molecules. We have derived analytical expressions for the reaction rates and shown that we match both the mean binding time and the mean rebinding time for $h^*_{\infty,g} \leqslant h \leqslant h^*_\infty$. For $h > h^*_\infty$, the gRDME and the sRDME agree.

We have studied the accuracy of the gRDME in two numerical examples. In the first example we show that we not only match the mean rebinding time for $h^*_{\infty,g} \leqslant h \leqslant h^*_\infty$, but also obtain a good match between the rebinding-time distributions at the two scales. In the second example we consider a system that cannot be accurately simulated with the sRDME, as the mesh resolution required is below the fundamental lower limit h^*_∞. We show that with the gRDME we are able to simulate the system to a high accuracy, and we show that we obtain convergence to the microscopic simulations with decreasing mesh size h.

ACKNOWLEDGMENTS

This work was funded by NSF Grant No. DMS-1001012, NIGMS of the NIH under Grant No. R01-GM113241-01, Institute of Collaborative Biotechnologies Grant No. W911NF-09-D-0001 from the U.S. Army Research Office, NIBIB of the NIH under Grant No. R01-EB014877-01, and U.S. DOE Grant No. DE-SC0008975.

[1] M. J. Lawson, B. Drawert, M. Khammash, and L. Petzold, Spatial stochastic dynamics enable robust cell polarization, PLoS Comput. Biol. **9**, e1003139 (2013).
[2] M. Howard and A. D. Rutenberg, Pattern Formation Inside Bacteria: Fluctuations Due to the Low Copy Number of Proteins, Phys. Rev. Lett. **90**, 128102 (2003).
[3] J. Elf and D. Fange, Noise induced Min phenotypes in E. coli, PLoS Comput. Biol. **2**, e80 (2006).
[4] M. Sturrock, A. Hellander, A. Marsavinos, and M. Chaplain, Spatial stochastic modeling of the hes1 pathway: Intrinsic noise can explain heterogeneity in embryonic stem cell differentiation, J. Roy. Soc. Interface **10**, 20120988 (2013).
[5] M. Sturrock, A. Hellander, S. Aldakheel, L. Petzold, and M. Chaplain, The role of dimerisation and nuclear transport in the hes1 gene regulatory network, Bull. Math. Biol. **76**, 766 (2013).
[6] K. Takahashi, S. Tănase-Nicola, and P. R. ten Wolde, Spatio-temporal correlations can drastically change the response of a MAPK pathway, Proc. Natl. Acad. Sci. USA **107**, 2473 (2010).
[7] J. Elf and M. Ehrenberg, Spontaneous separation of bi-stable biochemical systems into spatial domains of opposite phases, Syst. Biol. **1**, 230 (2004).
[8] B. Drawert, S. Engblom, and A. Hellander, URDME: A modular framework for stochastic simulation of reaction-transport processes in complex geometries, BMC Syst. Biol. **6**, 76 (2012).
[9] www.pyurdme.org.
[10] I. Hepburn, W. Chen, S. Wils, and E. De Schutter, STEPS: Efficient simulation of stochastic reaction-diffusion models in realistic morphologies, BMC Syst. Biol. **6**, 36 (2012).
[11] J. Hattne, D. Fange, and J. Elf, Stochastic reaction-diffusion simulation with MesoRD, Bioinformatics **21**, 2923 (2005).
[12] M. Tomita, K. Hashimoto, K. Takahashi, T. S. Shimizu, Y. Matsuzaki, F. Miyoshi, K. Saito, S. Tanida, K. Yugi, J. C. Venter, and C. A. Hutchison, E-cell: Software environment for whole-cell simulation, Bioinformatics **15**, 72 (1999).
[13] M. v. Smoluchowski, Versuch einer mathematischen Theorie der Koagulationskinetik kolloider Lösungen, Z. Phys. Chem. **92**, 129 (1917).
[14] S. S. Andrews, N. J. Addy, R. Brent, and A. P. Arkin, Detailed simulations of cell biology with Smoldyn 2.1, PLoS Comput. Biol. **6**, e1000705 (2010).
[15] R. A. Kerr, T. M. Bartol, B. Kaminsky, M. Dittrich, J.-C. J. Chang, S. B. Baden, T. J. Sejnowski, and J. R. Stiles, Fast Monte Carlo simulation methods for biological reaction-diffusion systems in solution and on surfaces, SIAM J. Sci. Comput. **30**, 3126 (2008).
[16] S. Hellander, A. Hellander, and L. R. Petzold, Reaction-diffusion master equation in the microscopic limit, Phys. Rev. E **85**, 042901 (2012).
[17] S. Hellander, A. Hellander, and L. R. Petzold, Reaction rates for mesoscopic reaction-diffusion kinetics, Phys. Rev. E **91**, 023312 (2015).
[18] S. Isaacson, A convergent reaction-diffusion master equation, J. Chem. Phys. **139**, 054101 (2013).
[19] D. Fange, O. G. Berg, P. Sjöberg, and J. Elf, Stochastic reaction-diffusion kinetics in the microscopic limit, Proc. Natl. Acad. Sci. USA **107**, 19820 (2010).

[20] M. Doi, Second quantization representation for classical many-particle system, J. Phys. A: Math. Gen. **9**, 1465 (1976).
[21] J. C. Jaeger and H. S. Carslaw, *Conduction of Heat in Solids* (Oxford University Press, New York, 1959).
[22] S. Hellander and P. Lötstedt, Flexible single molecule simulation of reaction-diffusion processes, J. Comput. Phys. **230**, 3948 (2011).
[23] J. S. van Zon and P. R. ten Wolde, Green's-function reaction dynamics: A particle-based approach for simulating biochemical networks in time and space, J. Chem. Phys. **123**, 234910 (2005).
[24] J. S. van Zon and P. R. ten Wolde, Simulating Biochemical Networks at the Particle Level and in Time and Space: Green's-Function Reaction Dynamics, Phys. Rev. Lett. **94**, 128103 (2005).
[25] S. Engblom, L. Ferm, A. Hellander, and P. Lötstedt, Simulation of stochastic reaction-diffusion processes on unstructured meshes, J. Sci. Comput. **31**, 1774 (2009).
[26] E. W. Montroll and G. H. Weiss, Random walks on lattices. II, J. Math. Phys. **6**, 167 (1965).
[27] E. W. Montroll, Random walks on lattices. III. Calculation of first-passage times with application to exciton trapping on photosynthetic units, J. Math. Phys. **10**, 753 (1969).
[28] F. C. Collins and G. E. Kimball, Diffusion-controlled reaction rates, J. Colloid Sci. **4**, 425 (1949).
[29] N. Agmon and A. Szabo, Theory of reversible diffusion-influenced reactions, J. Chem. Phys. **92**, 5270 (1990).